THE JOURNAL OF BIOLOGICAL CHEMISTRY Vol. 272, No. 27, Issue of July 4, pp. 17118–17125, 1997
Printed in U.S.A.

Paclitaxel-resistant Human Ovarian Cancer Cells Have Mutant β-Tubulins That Exhibit Impaired Paclitaxel-driven Polymerization*

(Received for publication, January 30, 1997, and in revised form, March 26, 1997)

Paraskevi Giannakakou‡, Dan L. Sackett‡, Yoon-Koo Kang§, Zhirong Zhan‡, Jeroen T. M. Buters¶, Tito Fojo‡‖, and Marianne S. Poruchynsky‡

From the ‡Medicine Branch, Division of Clinical Sciences, NCI, National Institutes of Health, Bethesda, Maryland 20892, the §Division of Hematology/Oncology, Korea Cancer Center Hospital, Seoul 139-240, Korea, and the ¶Laboratory of Molecular Carcinogenesis, NCI, National Institutes of Health, Bethesda, Maryland 20892

Acquired resistance to paclitaxel can be mediated by P-glycoprotein or by alterations involving tubulin. We report two paclitaxel-resistant sublines derived from 1A9 human ovarian carcinoma cells. Single-step paclitaxel selection with verapamil yielded two clones that are resistant to paclitaxel and collaterally sensitive to vinblastine. The resistant sublines are not paclitaxel-dependent, and resistance remained stable after 3 years of drug-free culture. All cell lines accumulate [^{3}H]paclitaxel equally, and no *MDR-1* mRNA was detected by polymerase chain reaction following reverse transcription. Total tubulin content is similar, but the polymerized fraction increased in parental but not in resistant cells following the paclitaxel addition. Purified tubulin from parental cells demonstrated paclitaxel-driven increased polymerization, in contrast to resistant cell tubulin, which did not polymerize under identical conditions. In contrast, epothilone B, an agent to which the resistant cells retained sensitivity, increased assembly. Comparable expression of β-tubulin isotypes was found in parental and resistant cells, with predominant expression of the M40 and β2 isotypes. Sequence analysis demonstrated acquired mutations in the M40 isotype at nucleotide 810 (T → G; Phe^{270} → Val) in 1A9PTX10 cells and nucleotide 1092 (G → A; Ala^{364} → Thr) in 1A9PTX22 cells. These results identify residues β270 and β364 as important modulators of paclitaxel's interaction with tubulin.

Paclitaxel (PTX)[1] is a complex diterpene (1), active against a broad range of human tumors, including ovarian and breast carcinomas (2–4). The primary target of PTX is the microtubule (MT), which is vital for mitosis, motility, secretion, and proliferation (5). PTX stabilizes MTs by disrupting the dynamic equilibrium between soluble tubulin dimers and their polymerized form (6) and is a potent inhibitor of chromosome replication, blocking cells in the late G_2 or mitotic phases of the cell cycle (7–9).

Resistance to PTX has been shown to be mediated by the drug efflux pump, P-glycoprotein, but could also result from alterations in its intracellular target, tubulin. Although precise molecular alterations in MTs have not been identified, several mechanisms have been proposed. These include decreased tubulin (10), point mutations as evidenced by altered migration of α- or β-tubulin on two-dimensional SDS-polyacrylamide gel electrophoresis (11–13), differential expression of β-tubulin isotypes (14–17), and acetylation of α-tubulin (18).

To further elucidate the mechanism of action of PTX and to investigate mechanisms of PTX resistance other than those mediated by Pgp, we have isolated two PTX-resistant sublines derived from a human ovarian carcinoma cell line. Selected in the presence of the Pgp antagonist, verapamil, resistant cells do not express Pgp, but they exhibit a stable PTX-resistant phenotype. Compared with parental cells, resistant cells display defective PTX-driven tubulin polymerization both in intact cells and *in vitro* using purified tubulin. No differences are observed in the amount of total tubulin or in the relative level of expression of the β-tubulin isotypes. However, two different point mutations in β-tubulin were identified in the resistant cells. These results provide the first demonstration of tubulin point mutations in PTX-resistant cell lines and introduce a novel molecular mechanism of PTX resistance.

EXPERIMENTAL PROCEDURES

Materials—PTX, its C-2 analog 2-debenzoyl-2-meta-azidobenzoylpaclitaxel (19), and epothilone B (EPO B) were obtained from the Drug Synthesis and Chemistry Branch of NCI, National Institutes of Health. Vinblastine was from Sigma, and verapamil was from Knoll pharmaceuticals. Mouse monoclonal IgG antibodies against chick brain α-tubulin or rat brain β-tubulin were from Sigma. Horseradish peroxidase-conjugated sheep anti-mouse Ig antibody was from Amersham Corp. ECL (enhanced chemiluminescence) Western blotting detection reagents were from Amersham. The *Taq* DyeDeoxy® terminator Cycle Sequencing kit was from Applied Biosystems, Inc., the PCR Select-III spin columns were from 5 Prime → 3 Prime, Inc., and the Centri-Sep spin purification columns were from Princeton Separations. T_4 polynucleotide kinase was from Life Technologies, Inc., and [γ-^{32}P]ATP was from Amersham. All other chemicals were of reagent grade and were from Sigma.

Cell Culture—The 1A9 cell line is a clone of the human ovarian carcinoma cell line, A2780 (20). The two resistant sublines, 1A9PTX10 and 1A9PTX22, were isolated as individual clones in a single step selection, by exposing 1A9 cells to 5 ng/ml PTX in the presence of 5 μg/ml verapamil, a Pgp antagonist. After an initial expansion in 5 ng/ml PTX, the concentration of PTX was gradually increased to 15 ng/ml. The cells utilized in these studies were maintained in 15 ng/ml PTX and 5 μg/ml verapamil continuously. Drug was removed for 5–7 days prior to an experiment.

Cytotoxicity Assay—Cytotoxicity assays were performed in 96-well plates as described previously (21), by seeding 500 cells/well and incubating with cytotoxic agents for 4 days. The IC_{50} was defined as the dose of drug required to inhibit cell growth by 50%.

Tubulin Polymerization Assay—To quantitate tubulin polymerization, a simple assay was developed by modifying a method originally described by Minotti (10). Cells grown to confluency in 24-well plates were washed twice with phosphate-buffered saline and lysed at 37 °C for 5 min in the dark, with 100 μl of hypotonic buffer (1 mM $MgCl_2$, 2 mM

* The costs of publication of this article were defrayed in part by the payment of page charges. This article must therefore be hereby marked "*advertisement*" in accordance with 18 U.S.C. Section 1734 solely to indicate this fact.

‖ To whom correspondence should be addressed: Medicine Branch, DCS, NCI, NIH, Bldg. 10, Rm 12N226, 9000 Rockville Pike, Bethesda, MD 20892.

[1] The abbreviations used are: PTX, paclitaxel; Pgp, P-glycoprotein; MT, microtubule; EPO B, epothilone B; PCR, polymerase chain reaction; Mes, 2-(*N*-morpholino)ethanesulfonic acid.

EGTA, 0.5% Nonidet P-40, 2 mM phenylmethylsulfonyl fluoride, 200 units/ml aprotinin, 100 μg/ml soybean trypsin inhibitor, 5.0 mM ϵ-amino caproic acid, 1 mM benzamidine, and 20 mM Tris-HCl, pH 6.8) without or with 0.04–4 μg/ml PTX. The presence of PTX in the hypotonic buffer allowed the assay to be performed on a crude tubulin extract, eliminating factors such as drug uptake and metabolism as experimental variables. The lysates were transferred to 1.5-ml Eppendorf tubes, and each well was rinsed with 100 μl of hypotonic buffer. Following a brief but vigorous vortex, the samples were centrifuged at 14,000 rpm for 10 min at room temperature. The 200-μl supernatants containing soluble (cytosolic) tubulin were transferred to another Eppendorf tube separating them from the pellets containing polymerized (cytoskeletal) tubulin. The pellets were resuspended in 200 μl of hypotonic buffer.

The cytosolic and cytoskeletal fractions were each mixed with 70 μl of 4 × SDS-polyacrylamide gel electrophoresis sample buffer (45% glycerol, 20% β-mercaptoethanol, 9.2% SDS, 0.04% bromphenol blue, and 0.3 M Tris-HCl, pH 6.8) and heated at 95 °C for 5–10 min. Twenty microliters of each sample were analyzed by immunoblotting, and ECL was quantitated by densitometry. The percentage of polymerized tubulin was determined by dividing the densitometry value of polymerized tubulin by the total tubulin content (the sum of the densitometry values of soluble and polymerized tubulin). The distribution of tubulin between the soluble and polymerized fractions could be altered to some extent by experimental conditions. Increased temperature during harvesting increased the polymerized fraction, so care was taken to maintain consistency, and each experiment was performed with appropriate controls.

Mixing Experiment—For the mixing experiment, parental 1A9 and clone 1A9PTX10 cells were lysed in hypotonic buffer, without or with 40 μg/ml PTX, for 5 min at 37 °C. Whole cell lysate from parental 1A9 cells was added to clone 1A9PTX10 lysate at varying ratios ranging from 1:1 to 1:19 (parental:resistant) at room temperature. The mixed lysates were incubated at 37 °C for another 5 min, and then the extent of tubulin polymerization was assessed using the tubulin polymerization assay described above.

Tubulin in Vitro Polymerization Assay—Tubulin was purified from the cell lines as described previously (22). The final preparation of polymerization-competent tubulin was >95% pure by SDS gel analysis. *In vitro* polymerization of pure tubulin was assayed as described previously (23). The concentration of tubulin was 7.5 μM, the concentration of GTP was 0.1 mM, and the concentration of PTX and epothilone B was 1 μM in all cases.

Electron Microscopy—Fifty-microliter aliquots were removed from polymerization reactions at steady state using pipette tips with a wide orifice to avoid shearing. These samples were applied without fixation to carbon/formvar-coated grids and allowed to adsorb for 30 s. After draining, the grids were negative stained with 1% uranyl acetate and air-dried.

Quantitative PCR—Quantitative PCR for β-tubulin isotypes was performed as described previously (24). Specific primers for each β-tubulin isotype: M40 (class I), β9 (class II), β4 (class III), 5β (class IVa), β2 (class IVb), were utilized as described previously (16) (arabic numerals refer to the human gene, and roman numerals refer to the protein isotype class (25)). In the case of the β4 (class III) forward primer, the bases CAC were added at the 3′-end. The primers utilized in the quantitative PCR, with the exception of the β9 primers, span one or two introns. This allows for discrimination between RNA and DNA products. For β9, PCR was performed without reverse transcription, and no product was obtained, confirming the absence of DNA contamination.

Sequence Analysis of β-Tubulin—For PCR amplification and sequencing of β2 or M40 isotypes, four overlapping sets of primers for each isotype were used, as summarized in Table I. Despite the sequence identity of β2 and M40, the primers were designed to be specific for each isotype, using published sequence data for M40 and β2 (26). The GenBank™ accession numbers for β2 and M40 isotypes are X02344 and J00314, respectively. PCR-amplified cDNA was purified with PCR Select-III spin columns and directly sequenced with the *Taq* DyeDeoxy® terminator cycle sequencing kit following the manufacturer's instructions (Applied Biosystems, Inc.). The primers used for sequencing were the same primers used for PCR amplification. The reaction products were purified with Centri-Sep spin purification columns, electrophoresed on 48-cm/4.75% polyacrylamide/urea gels, and analyzed by an automated DNA sequencing system (model 373A; Applied Biosystems, Inc.).

Oligonucleotide Hybridization—Oligonucleotide hybridization was performed using probes specific for the mutations found in the resistant sublines. PCR amplification of 1 μg of RNA after reverse transcription or PCR amplification of 1 μg of DNA from the three cell lines was performed. Equal amounts of the products were applied to nitrocellulose membrane in each of two adjacent slots. For the β270 mutation (nucleotide 810) of the M40 isotype, set 3 primers were used, as described in Table I. For the β364 mutation (nucleotide 1092) of the M40 isotype, the forward primer was the primer of set 4 (Table I), and the reverse primer was 5′-^{1248}CGACCTCGTCTCTGAGTATC^{1267}-3′.

To avoid the possibility of DNA contamination in the RNA, the RNA was treated with DNase (RNase-free) for 1 h at 37 °C and 5 min at 75 °C, prior to PCR. Subsequently, the absence of DNA contamination was confirmed by PCR amplification without the reverse transcription step.

Oligonucleotide probes specific for each of the mutations were 5′-phosphorylated with [γ-^{32}P]ATP and T_4 polynucleotide kinase. These probes were ^{801}ATGCCTGGC*X*TTGCCCCTCT^{819} (where *X* represents T for the wild type and G for the mutant) and ^{1080}GGCCTCAAGATG*X*-CAGTCACC^{1098} (where *X* represents G for the wild type and A for the mutant). Fifty and five nanograms of oligonucleotides complementary to each probe were slotted below the PCR products as controls. Hybridizations and washes were carried out as described by Mullis *et al.* (27).

TABLE I
Set of primers for PCR amplification and nucleotide sequencing of β2 and 40 β-tubulin isotypes

Primer	Sequence
Set 1	
Forward (19–35)	
β2	TTGCAGGCCGGGCAGTG
M40	A-C------T--T--A--[a]
Reverse (357–377)	
β2	GTTGTGAGAAAGGAGGCTGA
M40	--G--AC-G--------A--
Set 2	
Forward (283–301)	
β2	AGTGGTGCTGGGAACAACT
M40	TC---G--A--T-------
Reverse (628–648)	
β2	ATTTGCTTCAGAACCCTAAAG
M40	--C------C-C--T--G---
Set 3	
Forward (574–593)	
β2	CTCGTAGAAAACACAGACGA
M40	T-G-----G--T--T--T--
Reverse (1077–1095)	
β2	GGGGCTAAAATCCGCC
M40	T--C--C--GA-A-T-
Set 4	
Forward (985–1008)	
β2	CAAATGCTTAATGTCCAAAACAAA
M40	--G--------C--G--G-----G
Reverse (1327–3′ UTR)[b] β2	GAGGTGGCCTAGAGCCCT
Reverse (1322–3′ UTR)[b] M40	AAGAGGAGGCCTAGAGCCTT

[a] Residues with identity between β2 and M40 β-tubulin isotype, are designated by a hyphen.

[b] UTR, untranslated region. The coding sequence for the reverse primer for the β2 isotype ends at nucleotide 1335, and for the M40 isotype it ends at nucleotide 1332.

RESULTS

Resistance Profile of 1A9 and PTX-resistant Cells—The drug sensitivity of parental 1A9 and the PTX-resistant cells is shown in Table II. The resistant sublines were 24-fold more resistant to PTX and collaterally sensitive to vinblastine. They also exhibited slight cross-resistance (1.4–3-fold) to the PTX analog, 2-debenzoyl-2-meta-azidobenzoylpaclitaxel and to EPO B, a natural product with a mechanism of action similar to that of PTX but with a different chemical structure (28).

Effect of PTX on Tubulin Polymerization—Initial experiments showed that the two PTX-resistant sublines do not express *MDR-1*, that their intracellular PTX accumulation is comparable with that of the parental cell line, and that the total tubulin levels are similar to the levels observed in the parental cell line (data not shown). These findings led us to examine the effects of PTX on the relative levels of polymerized and soluble tubulin in parental and resistant cells. Cells were lysed for 5 min at 37 °C with a hypotonic buffer without or with

TABLE II
Cytotoxicity profile of 1A9 and 1A9PTX^R cells

Drugs	1A9 IC_{50}[a]	PTX 10		PTX 22	
		IC_{50}	RR[b]	IC_{50}	RR[b]
Paclitaxel	2	47	24	48	24
Vinblastine	3.5	1.6	0.5	1.4	0.4
Epothilone B	0.25	0.7	2.8	0.35	1.4
m-N_3-PTX[c]	0.03	0.09	3	0.09	3

[a] IC_{50}, drug concentration (in nM) at which cell growth is inhibited by 50%.
[b] RR, relative resistance = IC_{50} for resistant cell line/IC_{50} for parental cell line.
[c] m-N_3-PTX, 2-debenzoyl-2-*meta*-azidobenzoylpaclitaxel.

0.04–4 μg/ml PTX, and the levels of polymerized and soluble tubulin were assessed (Fig. 1*A*). To maximize the sensitivity for detecting polymerization, we chose experimental conditions that gave a minimal basal level of polymerization. In the absence of PTX, the majority of tubulin was found in the soluble form (10), and the ratios of polymerized (*P*) and soluble (*S*) tubulin were similar for all three cell lines. With increasing doses of PTX (0.04–4 μg/ml), tubulin polymerization increased in the parental 1A9 cells but not in the two resistant sublines.

Stability of PTX Resistance Phenotype—To examine the stability of the phenotype, the resistant clones were cultured in the absence of PTX and verapamil in an attempt to obtain drug-sensitive revertants. However, after 3 (PTX10) and 2 (PTX22) years of growth in drug-free media, reversal of the resistant phenotype had not occurred, as assessed by the polymerization analysis shown in Fig. 1*B*. Increasing PTX concentrations (0.04–4 μg/ml) resulted in a dose-dependent increase of tubulin polymerization in the parental, but not in the 1A9PTX10 and 1A9PTX22 cells that had been maintained drug-free for 3 and 2 years, respectively.

Mixing Experiment—To examine whether a soluble factor needed for tubulin polymerization was missing in the resistant sublines, we performed a mixing experiment. Whole cell lysate from parental 1A9 cells was added to lysate from resistant cells at varying ratios ranging from 1:1 to 1:19 (parental:resistant), to examine if parental cell lysate could induce polymerization in the resistant clone lysate. The data presented are from duplicate samples (Fig. 2). The *upper panel* shows the results when harvesting, mixing of lysates, and incubation were performed in the absence of PTX. Only a very small fraction of tubulin was polymerized (*P lanes*). The *lower panel* shows the results in the presence of PTX. As was demonstrated in Fig. 1*A*, in parental 1A9 cells, most of the tubulin is present in the polymerized form, in contrast to 1A9PTX10 cells, where the majority of tubulin is in the soluble form. Furthermore, the addition of lysate from parental cells did not induce polymerization of tubulin from the PTX-resistant clone. In each combination, the amount of polymerized tubulin in the *P lanes* reflects the contribution only from parental cells, as evidenced by the reduction in the amount of polymerized tubulin observed as the fraction of parental cell lysate decreases. Thus, there is no induction of polymerization or recruitment of tubulin from the resistant clone, even in the presence of some polymerized tubulin. Similar results were also found for the clone 1A9PTX22 (data not shown).

In Vitro Tubulin Polymerization with PTX and Epothilone B—To corroborate and extend the biochemical evidence presented thus far, tubulin was purified from parental and resistant cells to confirm that the differences were secondary to specific alterations in the tubulin molecule. As shown in Fig. 3*A*, 1 μM PTX stimulated polymerization of parental cell tubulin to about the same extent as rat brain tubulin. In contrast, tubulin from the resistant cells exhibited impaired PTX-driven polymerization. Tubulin from clone 1A9PTX10 polymerized to a level less than half of parental, and tubulin from clone

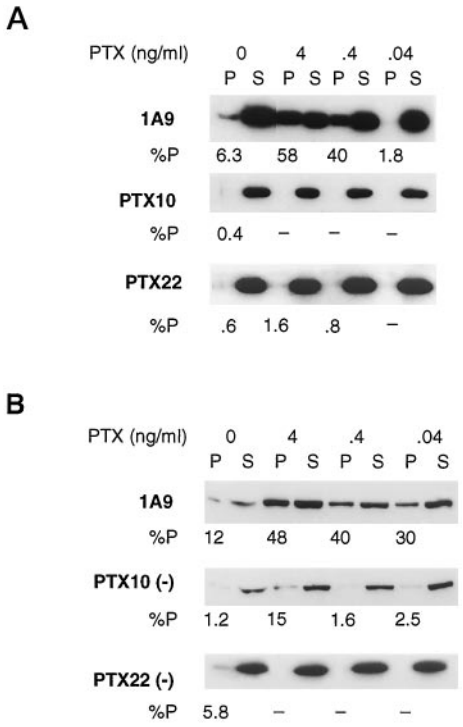

FIG. 1. **Effect of PTX on tubulin polymerization in 1A9 and PTX-resistant cells.** *A*, drug-sensitive parental 1A9 and the resistant clones PTX10 and PTX22 were lysed with a hypotonic buffer without (0) or with 0.04–4 μg/ml PTX, for 5 min at 37 °C. Following cell lysis the polymerized (*P*) and the soluble (*S*) protein fractions were separated by centrifugation, and each fraction was resolved on adjacent lanes by electrophoresis. After transfer, the filter was probed with an antibody against α-tubulin. The resistant cells were maintained in drug-free medium for 1 week prior to the experiments. *B*, the same experiment was performed with the two resistant clones that had been maintained in drug-free medium for 3 (PTX10(−)) and 2 years (PTX22(−)), respectively. The percentage of polymerized tubulin (%*P*) was determined by dividing the densitometric value of polymerized tubulin by the total tubulin content (the sum of *P* plus *S*).

1A9PTX22 failed to polymerize at all. Furthermore, EPO B polymerized tubulin from the two resistant clones to the same extent as parental cell tubulin (Fig. 3*B*), consistent with the cytotoxicity results (Table II), demonstrating low to absent cross-resistance to EPO B. Fig. 3*C* demonstrates that the turbidity increase shown in Fig. 3*A* results from normal microtubule structures that exhibit typical morphology and dimensions. This is illustrated by electron microscopy of a negatively stained preparation of parental cell tubulin following the addition of PTX. It is important to emphasize that the purified tubulins were unimpaired in their intrinsic ability to polymerize, since the final step in purification isolated protein that polymerized at 37 °C and depolymerized on ice.

Expression of β-Tubulin Isotypes in Parental and Resistant Cells by Quantitative PCR—Our studies suggested alterations in tubulin as the cause for the defect in PTX-driven tubulin

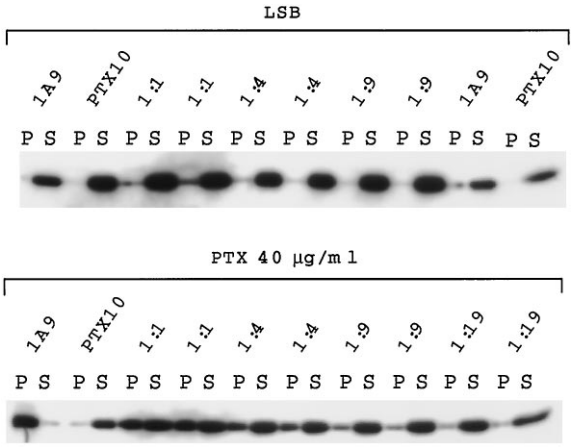

FIG. 2. **Mixing experiment.** Drug-sensitive parental 1A9 and 1A9PTX10 cells were harvested by adding hypotonic buffer without (*LSB*) or with 40 μg/ml PTX for 5 min at 37 °C. After harvesting, the whole cell lysate from the parental cell line was added to that of the resistant subline at different ratios ranging from 1:1 to 1:19 (1A9:PTX10), and incubated for an additional 5 min at 37 °C. The polymerized (*P*) and soluble (*S*) protein fractions were separated by centrifugation, and each fraction was resolved on adjacent lanes by electrophoresis. After transfer, the filter was probed with an antibody to α-tubulin. The results are presented as duplicate samples.

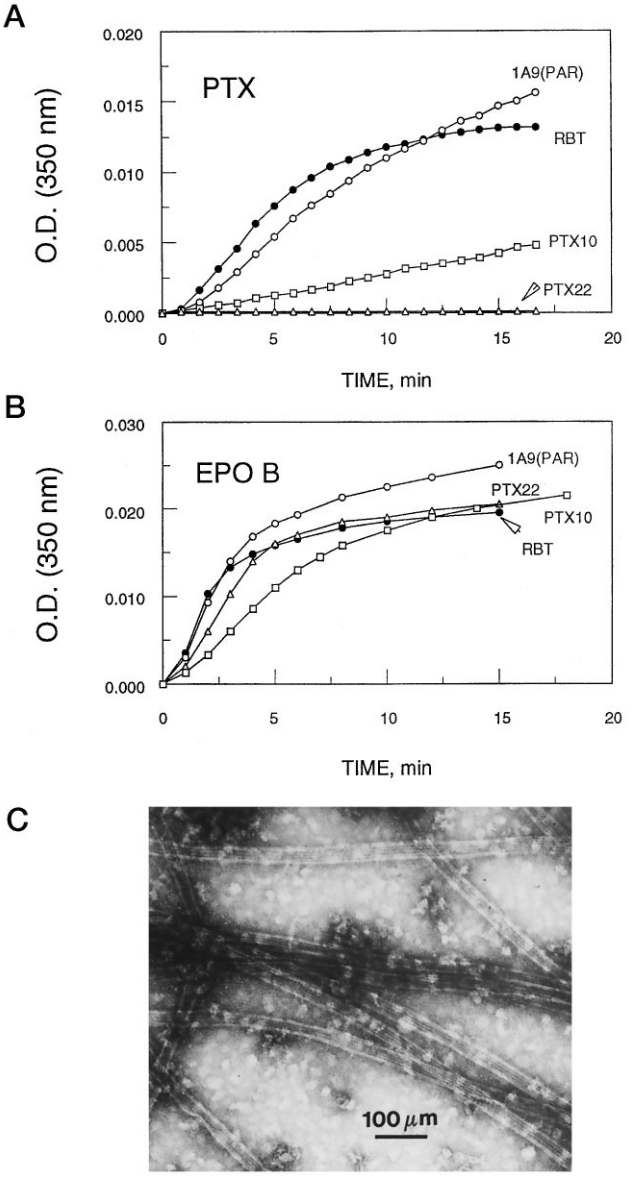

FIG. 3. ***In vitro* tubulin polymerization with PTX and EPO B.** *A* and *B*, polymerization of pure tubulin from rat brain, 1A9 parental, 1A9PTX10 and 1A9PTX22 cells in Mes assembly buffer was followed by the light scattering-induced increase in optical density at 350 nm at 37 °C. The concentration of tubulin was 7.5 μM, the concentration of GTP was 0.1 mM, and that of PTX (*A*) and EPO B (*B*) was 1 μM in all cases. *C*, electron microscopy of a negative stained preparation of parental cell tubulin polymerized with PTX as in *A*, showing normal microtubule structures.

polymerization. These alterations could be secondary to differences in the coding sequence or post-translational modifications.

The expression of five β-tubulin isotypes was examined by quantitative PCR (Fig. 4*A*). These isotypes were M40 (class I), β2 (class IVb), β9 (class II), β4 (class III), and 5β (class IVa). PCR amplification was performed for 30 cycles, with different dilutions used for each isotype to ensure that amplification was in the linear range. Tubulin isotype levels were normalized to the input RNA for each cell line, and their expression relative to that of parental cells was determined (Fig. 4*B*). Similar results were obtained when the isotype levels were normalized to β2-microglobulin (data not shown). A 1.4–1.8-fold increase of M40 was observed in the two resistant clones, while a 20–30-fold decrease of 5β was observed for clones 1A9PTX10 and 1A9PTX22, respectively. The very low levels of 5β isotype precluded accurate densitometry, and argue against a significant contribution of this isotype in the tubulin behavior observed in these cells.

Fig. 4, *C* and *D*, presents the relative expression of the five isotypes in parental 1A9 cells. *Panel C* presents the results of PCR amplification for 30 cycles, using different amounts of RNA as indicated for each isotype. The M40 isotype was detected with the lowest amount of RNA, indicating it is the most prevalent isotype. The β2 isotype was detected with the second lowest amount of RNA, indicating that its expression is lower than M40 but higher than the other three isotypes. By quantitating the products by densitometry and correcting for product size, the relative levels of expression of the five isotypes were calculated. This is an approximation, since the primers utilized could amplify with different efficiencies. The results are presented in Fig. 4*D*, where the relative percentage of each isotype in 1A9 cells is shown. Assuming comparable efficiencies of translation and protein stability, the percentage of each isotype in parental cells is as follows: M40, 84%; β2, 11%; β9, 4.2%; β4, 0.5%; and 5β, 0.3%. Although these calculations are approximations, they suggest that the predominant isotypes are M40 and β2.

Sequencing of β2 and M40 β-Tubulin Isotypes—Since the PTX phenotype could not be explained by changes in the relative levels of β-tubulin isotypes, sequencing of the two predominant isotypes, M40 and β2, was performed. We reasoned that a mutation in a predominant isotype would be more likely to confer resistance. The cDNA sequence of the β2 isotype was "wild type" in all cell lines, both by automated sequencing and by subcloning and manual sequencing of three or four individual colonies for each cell line and each set of primers. In contrast, two distinct point mutations were identified in the cDNA of the M40 isotype, one in each of the two PTX-resistant sublines (Fig. 5). In clone 1A9PTX10, a T → G substitution in nucleotide 810 changed amino acid 270 from phenylalanine (TTT) to valine (GTT). In clone 1A9PTX22, a G → A substitution in nucleotide 1092 changed amino acid 364 from alanine (GCA) to threonine (ACA). Both substitutions were each present as a single peak in the sequence analysis (not shown), indicating expression of mRNA with wild type sequence could not be detected.

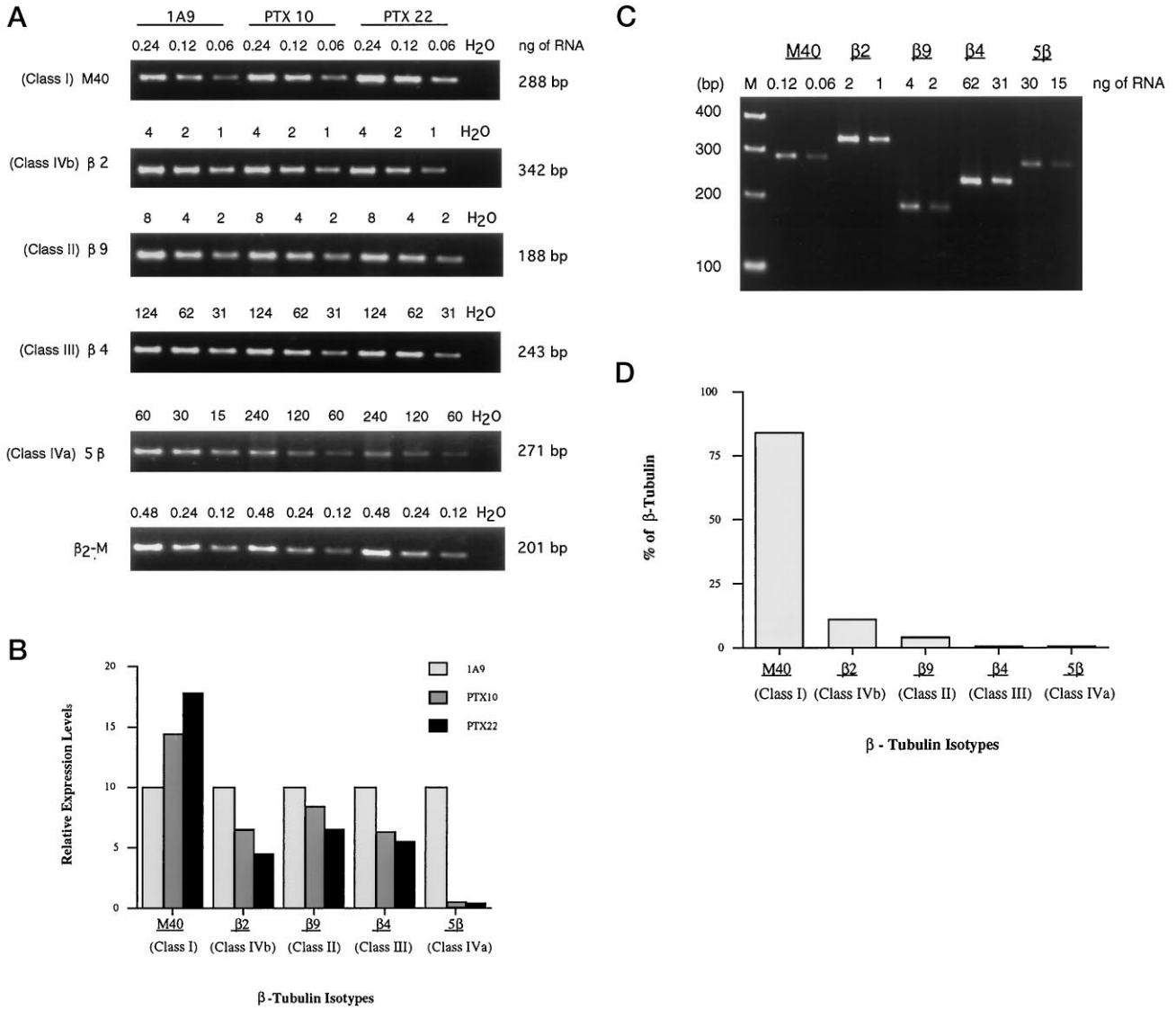

FIG. 4. **Expression of β-tubulin isotypes.** *A*, the expression of β-tubulin isotypes was examined in 1A9 and resistant cells by quantitative PCR, following reverse transcription. Different amounts of RNA were utilized as indicated to ensure that samples were in the exponential range of amplification. *B*, *bar graph* representation of the results displayed in *A*. The level of each β-tubulin isotype in the 1A9 parental cells is arbitrarily given the value of 10, to compare the expression level in the two resistant sublines relative to that of the parental. These values were derived from the results in *A*, using 28 S as the standard. *C*, the expression of the five β-tubulin isotypes in 1A9 parental cells by quantitative PCR following reverse transcription. Different amounts of RNA were utilized, as indicated. *D*, *bar graph* representation of the results displayed in *C*. The total β-tubulin percentage of each of the five isotypes in parental 1A9 cells is presented. The percentage was calculated after quantitation of each PCR product by densitometry and correction for the product size, as described under "Results."

Oligonucleotide Hybridization—Oligonucleotide hybridization using two different probes spanning the regions containing the mutations was performed (Fig. 5). To examine both RNA and DNA, PCR products from both RNA (converted to cDNA) and DNA were obtained by PCR using primers flanking the mutations. The products were slotted and hybridized under identical conditions. As shown in Fig. 5, clone 1A9PTX10 expresses only the RNA with the acquired βF270V mutation, although it is heterozygous at the DNA level. A similar result for the βA364T mutation was observed for the 1A9PTX22 clone. These results confirm the presence of tubulin mutations in the PTX-resistant human ovarian carcinoma cell lines.

DISCUSSION

Drug resistance can originate through multiple mechanisms, such as changes in cellular drug uptake, metabolic drug deactivation, structural changes in the drug target, or changes in other cellular components that interact with the target (29). Some of these have been implicated in the emergence of resistance to paclitaxel. To identify mechanisms of PTX resistance other that those mediated by Pgp, we isolated PTX-resistant human ovarian carcinoma cell lines. Two resistant cell lines, derived from a subclone of the human ovarian carcinoma line, A2780, were characterized. These sublines were isolated in a single step by exposure to PTX in the presence of the Pgp antagonist, verapamil. Previous studies have shown that verapamil can negate the appearance of Pgp, resulting in the selection of cells that exhibit other mechanisms of drug resistance (30). The resistant cells are 24-fold more resistant to PTX, 1.4–3-fold more cross-resistant to either 2-debenzoyl-2-meta-azidobenzoylpaclitaxel or EPO B, and collaterally sensitive to vinblastine. Expression of *MDR-1* was not detectable, nor was PTX accumulation decreased in the resistant cells (data not shown). Thus, these cells provide a valid model of non-Pgp-mediated PTX resistance.

In contrast to other PTX selected cell lines that have been reported, the resistant cells described in this study are not

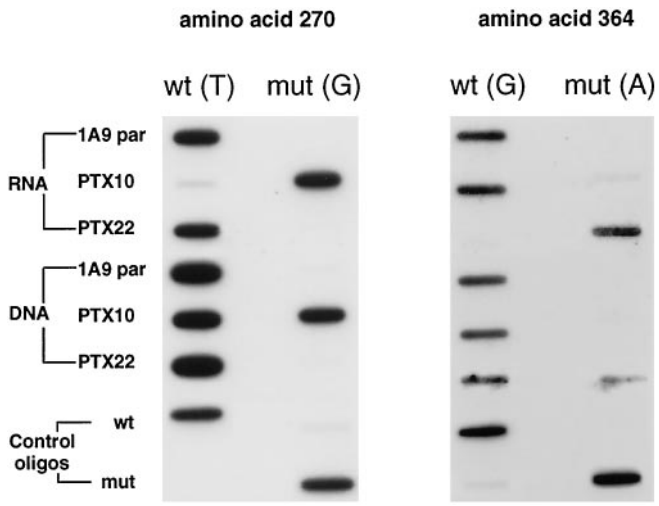

FIG. 5. **Oligonucleotide hybridization.** Independent experiments were performed for each mutation identified in β-tubulin. For each one, PCR products were obtained using primers spanning the mutation. The template was either RNA (converted to cDNA) or DNA. Equal amounts of PCR product from the three cell lines were slotted side by side on a nitrocellulose membrane. The membrane was divided into two equal halves, and each half was hybridized with an oligonucleotide probe containing either wild type (*wt*) or mutant (*mut*) sequences. After washing, the halves were brought together for the autoradiogram. Below the PCR products, 50 ng of primers complementary to each probe were slotted as controls. For each of the two probes, the nucleotide substitutions between the wild type and mutant sequences are shown in *parentheses*.

PTX-dependent for growth (18, 31). Their growth rate is similar in the absence and presence of PTX (data not shown). This indicates that the resistant phenotype protects MT function from PTX effects without altering MT function in the absence of PTX. Furthermore, the resistant phenotype remained stable in the absence of drug for 3 years.

Multiple changes in the PTX target, tubulin, have been reported in PTX-resistant cell lines. These include reduced total tubulin levels (10, 24), increased tubulin content (15), differential migration of α- or β-tubulin on two-dimensional polyacrylamide gel electrophoresis (11, 13), acetylation of α-tubulin (18), and increased expression of specific tubulin isotypes (14–17). In the present study, the total tubulin content of the resistant cells was similar to that of the parental cells (data not shown), and no differences in the acetylation of purified α-tubulin were observed (data not shown). Thus, we sought other explanation(s) for the origin of PTX resistance in these cells.

Since PTX promotes tubulin polymerization, we compared the relative ratios of soluble and polymerized tubulin in the resistant cells. In a first approximation, immunofluorescent microscopy revealed no difference in the amount of MTs between the 1A9 parental cells and the resistant cells (data not shown). These results were confirmed and extended using the tubulin polymerization assay. Although this method of evaluation was designed to measure the response to added PTX rather than steady-state polymerization, similar ratios of polymerized and soluble tubulin were obtained for untreated cells for each cell line. In contrast, in the presence of PTX, a dose-dependent tubulin polymerization was observed only in 1A9 parental cells. In addition, mixing cell lysates from parental and resistant cells did not induce polymerization of tubulin in the resistant cell lysates, nor did parental cell-derived polymers recruit tubulin from the resistant cell lysates. Moreover, the degree of PTX-induced polymerization of tubulin purified from the resistant clones was less than that of the tubulin from the parental cell or from rat brain. These data suggested that the primary defect was one of tubulin structure or composition.

Human genes coding for α- or β-tubulin constitute a multigene family of 15–20 members, several of which are pseudogenes (32, 33). Although there is some tissue specificity of isotype expression, the role of isotypes remains unclear (34). It has been reported that isotype composition can regulate MT dynamics *in vitro* (35); however, transfection experiments have shown that exogenous isotypes are incorporated into microtubule structures and appear to function interchangeably (36). There is also evidence that in the absence of a particular isotype, other isotypes are substituted without affecting normal function (36).

The demonstration of differential expression of tubulin isotypes in cell lines resistant to MT active agents (14–17) has prompted some authors to postulate this as a mechanism of PTX resistance. However, mutations in a tubulin isotype have not been excluded. Indeed, if an acquired mutation confers an advantage, prolonged selection might lead to its overexpression. This could manifest as altered isotype expression, although the selective advantage was conferred by the mutation and not by the native isotype.

In the present study, M40 isotype expression was increased about 1.5-fold; however, this data appeared inadequate to explain the 24-fold PTX resistance, although the isotype expression levels might contribute to the drug-resistant phenotype. The polymerization results using either cell lysates (Fig. 1) or purified tubulin (Fig. 3) indicate that parental tubulin and hence the mixture of isotypes present in parental tubulin polymerizes in response to added PTX. Therefore, it seemed unlikely that a 1.5-fold change or less in the level of any of these PTX-responsive isotypes would result in PTX resistance. Consistent with this, point mutations in β-tubulin were found in the class I isotype, M40, which represented the majority of total β-tubulin mRNA. These two mutations in independently selected cells were not identical. The M40 β270 mutation in clone 1A9PTX10, a T → G substitution in nucleotide 810, changed amino acid 270 from phenylalanine (TTT) to valine (GTT). The M40 β364 mutation in clone 1A9PTX22, a G → A substitution in nucleotide 1092, changed amino acid 364 from alanine (GCA) to threonine (ACA). The remainder of the M40 nucleotide sequence in both clones was consistently found to be identical to the parental sequence. These changes in β-tubulin most likely contribute to PTX resistance in these cells.

The oligonucleotide hybridization studies confirmed the expression of mutant β270 and β364 tubulins in the respective cell lines and demonstrated at the DNA level both wild type and mutant sequences. Interestingly, although an allele with wild type sequence was present in the DNA from both resistant sublines, only the mutant allele was expressed. This pattern of expression is under current investigation.

Two models of resistance mechanisms might explain the effects of these mutations. It is possible that the mutations alter the PTX binding site such that PTX binding is inhibited but MT function is unaffected in the absence of PTX. Alternatively, it is possible that the mutations could alter a region of tubulin important for dimer-dimer contacts in the MT polymer, weakening the interaction and producing less stable MT (37). The addition of PTX up to some threshold level would then produce more normal MT rather than the "hyperstabilized" MT produced with wild type tubulin.

We favor the first mechanism for several reasons. First, the resistant clones do not exhibit any MT defect in the absence of PTX, their growth rate is the same in the absence or presence of PTX, and they have doubling times similar to parental cells. It seems unlikely that the MT of these cells are hypostable. Second, hypostable MT should be made more normal by any MT-stabilizing drug, and these should confer similar relative

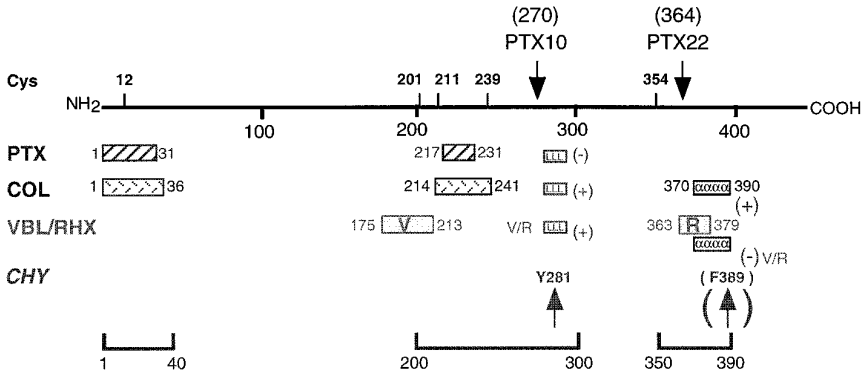

FIG. 6. **Schematic diagram of drug interaction sites on β-tubulin.** The *line* represents the sequence of β-tubulin with residue numbers indicated *below*. The position of the two mutations identified in the resistant cells are indicated by the *arrows above* the *line*. Cysteine residues referred to in the text are also indicated *above* the *line*. Three regions of the protein are involved in drug binding. These are indicated by *brackets* at the *bottom*, labeled *1–40*, *200–300*, and *350–390*. Particular features of each region are shown in the area *between* the *brackets* and the *sequence line*. The *filled bars* in this area refer to peptides identified in binding of the drugs labeled at the *left* of each *line*: PTX; colchicine (*COL*), and vinblastine/rhizoxin (*VBL/RHX*). The *open bars* with *letters* in them refer to structural features identified below. Peptides on the *VBL/RHX line* identified by interaction with vinblastine are labeled *V*, and those identified by rhizoxin are labeled *R*. The *line* labeled *CHY* identifies chymotrypsin cleavage sites in the native protein. Cleavage at Tyr^{281} occurs in a surface loop region indicated by the *bar* labeled *LLL*. This cleavage occurs in the absence of drug but can be enhanced (+) or inhibited (−) by drug binding. The *parenthesis* around the F389 site indicate that this site, which occurs at the end of a helical region indicated by the *bar* labeled *ααα*, only occurs after drug binding. Colchicine binding allows cleavage (+), while vinblastine/rhizoxin binding inhibits it (−). For further details, see the text.

resistance, but that was not observed. Rather, small structural changes in PTX altered the extent of resistance. For example, relative resistance to taxotere is less than half that to PTX (data not shown). The relative resistance to 2-debenzoyl-2-meta-azidobenzoylpaclitaxel, is even less. Moreover, the relative resistance to EPO-B, a MT-stabilizing agent structurally distinct from PTX that shares at least part of the same binding site, is less than 2-fold. Finally, the effects observed on cell growth paralleled an *in vitro* assay of drug-induced polymerization, using purified tubulin. PTX-induced polymerization of resistant tubulin was significantly decreased, but polymerization induced by EPO-B (Fig. 3) or 2-debenzoyl-2-meta-azidobenzoylpaclitaxel (38) was comparable with that obtained with parental or rat brain tubulin. Taken together, these results favor a mechanism based on weakening the interaction with the drug rather than weakening tubulin-tubulin interactions important to polymerization in the absence of drug.

Fig. 6 compares the sites of the mutations with other known drug interaction sites and maps the residues or peptides within β-tubulin shown to interact with PTX, colchicine, and vinblastine/rhizoxin. Vinblastine and rhizoxin share a binding site that is distinct from that for colchicine or PTX (39, 40). These sites/peptides were identified either by photoaffinity labeling or by induced structural changes. The sites identified by the latter, while not necessarily proximal to the binding site, are clearly affected by drug binding. Additionally, Fig. 6 shows the location of the two mutations identified in our study and the location of a loop exposed on the surface of the dimer. These features cluster in three regions of the sequence, indicated by *brackets* at the *bottom* of Fig. 6: the N-terminal 30 or 40 residues, a central region centered around residue 250, and a more C-terminal region containing residues 350–390. It is notable that these same regions comprise the sites of binding and action of agents that stabilize MT and enhance assembly, such as PTX, as well as of agents that inhibit assembly such as colchicine, vinblastine, and rhizoxin. These regions will be considered in turn.

The N-terminal region can be photolabeled by PTX and by colchicine. PTX, with the photoreactive group on the C-13 side chain, labels a peptide containing residues 1–31 (41). Photolabeling with colchicine also identifies an N-terminal peptide of 1–36 (42). Additionally, this peptide contains Cys^{12}, which is labeled by GTP (43). This residue, and the other cysteine residues indicated, will be discussed below.

The central region around residue 250 contains peptides labeled by all three groups of drugs, a loop sequence affected by drug binding, and the site of mutation in PTX10. PTX, with the photoreactive group on the C-2 side chain, labels a peptide containing residues 217–231 (44). Photolabeling with colchicine again labels an overlapping peptide, containing residues 214–241 (42). Vinblastine binding labels a site contained in residues 175–213 (45). This region also contains a surface-exposed, drug-sensitive loop sequence that contains the sole site of chymotrypsin cleavage in the native tubulin dimer, located after Tyr^{281} (46, 47). Exposure of this loop and consequent chymotryptic cleavage is enhanced by binding of colchicine, rhizoxin, or especially vinblastine (48) but is nearly completely suppressed by PTX (46). The finding that the PTX10 mutation locates to residue 270 in the center of this region and just N-terminal proximal to the loop sequence reinforces the importance of this region of the sequence to the binding of polymerization-modulating drugs indicated by previous data. It is notable that the PTX analog that most strongly reversed the resistant phenotype, 2-debenzoyl-2-meta-azidobenzoylpaclitaxel, is identical to the compound used to label this region (44).

The third, most C-terminal region, contains sites labeled by rhizoxin and colchicine and an amphipathic helical region strongly affected by drug binding. Photolabeling with a colchicine analog demonstrates that the A-ring of colchicine interacts with Cys^{354} (49). Rhizoxin photolabels a peptide containing residues 363–379 (50). This peptide overlaps a drug binding-sensitive amphipathic helical region containing residues ~370–390, whose carboxyl-terminal end is unfolded and made chymotrypsin-sensitive by colchicine (51). Unfolding is antagonized by vinblastine or rhizoxin, which promotes a form more tightly folded and protease-resistant at this site than the drug-free dimer (48). The location of the PTX22 mutation at residue 364 indicates that the PTX binding site contains contributions from this region of the sequence as well as the other two regions, as does the colchicine site.

In order for sequences from these three regions, very distant in linear sequence from each other, to contribute to the PTX binding site on β-tubulin, they clearly must be in close proximity in the folded form of native tubulin. Several lines of evidence, independent of data regarding PTX binding, allow us

to draw this conclusion. In addition to the clustering of data from multiple probes, the data from direct photolabeling with a single probe, colchicine, require that these sequences be close. Since colchicine labels peptides from all three regions, the contact sites within these peptides cannot be farther apart than the dimensions of the colchicine molecule, ~11 Å (42, 49). Additional compelling evidence comes from studies of cysteine cross-linking (52, 53). Using a bifunctional cross-linker with maximum span of ~9 Å, two cross-links could be formed in β-tubulin. One cross-link is between Cys^{12} (in the N-terminal region of Fig. 6) and Cys^{201} or Cys^{211} (in the central region of Fig. 6). The other is between Cys^{239} (in the central region) and Cys^{354} (in the C-terminal region). These cross-links are sensitive to drug binding; colchicine binding inhibits the Cys^{239}–Cys^{354} cross-link, whereas vinblastine enhances it while inhibiting the Cys^{12}–Cys^{201}/Cys^{211} cross-link. Thus, data independent of PTX binding indicate that these three regions of the β-tubulin sequence are close in the native protein and that the interactions between them are altered in subtle but important ways by the binding of MT-active drugs, including both assembly inhibiting and assembly-promoting agents. The identification in the present work of residues β270 and β364 as important modulators of the interaction of PTX with tubulin add to our understanding of this important binding site.

In summary, the present study describes the isolation and characterization of two PTX-resistant human ovarian carcinoma cell lines. This study is the first to identify specific point mutations in tubulin that result in PTX resistance in human cells. Our data have identified regions of β-tubulin whose alteration abrogates PTX action *in vitro* and confers cellular PTX resistance.

REFERENCES

1. Wani, M. C., Taylor, H. L., Wall, M. E., Coggon, P., and McPhail, A. T. (1971) *J. Am. Chem. Soc.* **93,** 2325–2327
2. Holmes, F. A., Walters, R. S., Theriault, R. L., Forman, A. D., Newton, L. K., Raber, M. N., Buzdar, A. U., Frye, D. K., and Hortobagyi, G. N. (1991) *J. Natl. Cancer Inst.* **83,** 1797–1805
3. McGuire, W. P., Rowinsky, E. K., Rosenshein, N. B., Grumbine, F. C., Ettinger, D. S., Armstrong, D. K., and Donehower, R. C. (1989) *Ann. Intern. Med.* **111,** 273–279
4. Rowinsky, E. K., and Donehover, R. C. (1995) *N. Engl. J. Med.* **332,** 1004–1014
5. Hyams, J. F., and Loyd, C. W. (1993) *Microtubules*, Wiley-Liss, New York
6. Horwitz, S. B., Cohen, D., Rao, S., Ringel, I., Shen, H. J., and Yong, C. P. (1993) *J. Natl. Cancer Inst.* **15,** 55–61
7. Horwitz, S. B. (1992) *Trends Pharmacol. Sci.* **13,** 134–136
8. Jordan, M., Toso, R. J., Thrower, D., and Wilson, L. (1993) *Proc. Natl. Acad. Sci. U. S. A.* **90,** 9552–9556
9. Schiff, P. B., and Horwitz, S. B. (1980) *Proc. Natl. Acad. Sci. U. S. A.* **77,** 1561–1565
10. Minotti, A. M., Barlow, S. B., and Cabral, F. (1991) *J. Cell Biochem.* **266,** 3987–3994
11. Cabral, F., Abraham, I., and Gottesman, M. M. (1981) *Proc. Natl. Acad. Sci. U. S. A.* **78,** 4388–4391
12. Schibler, M. J., Barlow, S. B., and Cabral, F. (1989) *FASEB J.* **3,** 163–168
13. Schibler, M. J., and Cabral, F. (1986) *J. Cell Biol.* **102,** 1522–1531
14. Dumontet, C., Duran, G. E., Steger, K. A., Beketic-Oreskovic, L., and Sikic, B. I. (1996) *Cancer Res.* **56,** 1091–1097
15. Haber, M., Burkhart, C. A., Regl, D. L., Madafiglio, J., Norris, M. D., and Horwitz, S. B. (1995) *J. Biol. Chem.* **270,** 31269–31275
16. Jaffrezou, J.-P., Dumontet, C., Derry, W. B., Duran, G. E., Chen, G., Tsuchiya, E., Wilson, L., Jordan, M.-A., and Sikic, B. I. (1995) *Oncol. Res.* **7,** 517–527
17. Ranganathan, S., Dexter, D. W., Benetatos, C. A., Chapman, A. E., Tew, K. D., and Hudes, G. R. (1996) *Cancer Res.* **56,** 2584–2589
18. Ohta, S., Kazuto, N., Ohmori, T., Funayama, Y., Ohira, T., Nakajiama, H., Adachi, M., and Saijo, N. (1994) *Jpn. J. Cancer Res.* **85,** 290–297
19. Chaudhary, A. G., Gharpure, M. M., Rimoldi, J. M., Chordia, M. D., Gunatilaka, A. A. L., Kingston, D. G. I., Grover, S., Lin, C. M., and Hamel, E. (1994) *J. Am. Chem. Soc.* **116,** 4097–4098
20. Eva, A., Robbins, K., Anderson, P., Srinivasan, A., Tronick, S., Reddy, E., Ellmore, N., Gallen, A., Lautenberger, J., Papas, T., Westin, E., Wong-Staal, F., Gallo, R., and Aaronson, S. (1982) *Nature* **295,** 116–119
21. Skehan, P., Storeng, R., Scudiero, D., Monks, A., McMahon, J., Vistica, D., Warren, J. T., Bokesch, H., Kenney, S., and Boyd, M. R. (1990) *J. Natl. Cancer Inst.* **82,** 1107–1112
22. Sackett, D. L. (1995) *Anal. Biochem.* **228,** 343–348
23. Gaskin, F., and Cautor, C. R. (1974) *J. Mol. Biol.* **89,** 737–758
24. Murphy, L. D., Herzog, C. E., Rudick, J. B., Fojo, A. T., and Bates, S. E. (1990) *Biochem. J.* **29,** 10351–10356
25. Sullivan, K. F., and Cleveland, D. W. (1986) *Proc. Natl. Acad. Sci. U. S. A.* **83,** 4327–4331
26. Lewis, S. A., Gilmartin, M. E., Hall, J. L., and Cowan, N. J. (1985) *J. Mol. Biol.* **182,** 11–20
27. Mullis, K., Faloona, F., Scharf, S., Saiki, R., Horn, G., and Erlich, H. (1986) *Cold Spring Harbor Symp. Quant. Biol.* **51,** 263–273
28. Bollag, D. M., McQueney, P. A., Zhu, J., Hensens, O., Koupal, L., Liesch, J., Goetz, M., Lazarides, E., and Woods, C. M. (1995) *Cancer Res.* **55,** 2325–2333
29. Pratt, W. B., Ruddon, R. W., Ensminger, W. D., and Maybaum, J. (1994) in *The Anticancer Drugs* (Pratt, W. B. and Ruddon, R. W., eds) pp. 50–66, Oxford University Press, New York
30. Chen, Y.-N., Mickley, L. A., Schwartz, A. M., Acton, E. M., Hwang, J., and Fojo, A. T. (1990) *J. Biol. Chem.* **265,** 10073–10080
31. Cabral, F. R., Brady, R. C., and Schibler, M. J. (1986) *Ann. N. Y. Acad. Sci.* **466,** 745–756
32. Cleveland, D. W., Lopata, M. A., MacDonald, R. J., Cowan, N. J., Rutter, W. J., and Kirschner, M. W. (1980) *Cell* **20,** 95–105
33. Wilde, C. D., Growther, C. E., Cripe, T. p., Gwo-Shu Lee, M., and Cowan, N. J. (1982) *Nature* **297,** 83–84
34. Luduena, R. F. (1993) *Mol. Biol. Cell* **4,** 445–457
35. Pand, D., Miller, H., Banerjee, A., Luduena, R. F., and Wilson, L. (1994) *Proc. Natl. Acad. Sci. U. S. A.* **91,** 11358–11362
36. Lewis, S. A., Gu, W., and Cowan, N. J. (1987) *Cell* **49,** 539–548
37. Cabral, F., and Barlow, S. B. (1989) *FASEB J.* **3,** 1593–1599
38. Sackett, D. L., Giannakakou, P., Poruchynsky, M., and Fojo, A. T. (1997) *Cancer Chemother. Pharmacol.* **40,** 228–232
39. Bai, R., Pettit, G. R., and Hamel, E. (1990) *J. Biol. Chem.* **265,** 17141–17149
40. Hamel, E. (1992) *Pharmacol. Ther.* **55,** 31–51
41. Rao, S., Krauss, N. E., Heerding, J. M., Swindell, C. S., Ringel, I., Orr, G. A., and Horwitz, S. B. (1994) *J. Biol. Chem.* **269,** 3132–3134
42. Uppuluri, S., Knipling, L., Sackett, D. L., and Wolff, J. (1993) *Proc. Natl. Acad. Sci. U. S. A.* **90,** 11598–11602
43. Shivanna, B. D., Mejillano, M. R., Williams, T. D., and Himes, R. H. (1993) *J. Biol. Chem.* **268,** 127–132
44. Rao, S., Orr, G. A., Chaudhary, A. G., Kingston, D. G. I., and Horwitz, S. B. (1995) *J. Biol. Chem.* **270,** 20235–20238
45. Rai, S. S., and Wolff, J. (1996) *J. Biol. Chem.* **271,** 14707–14711
46. Sackett, D. L., and Wolff, J. (1986) *J. Biol. Chem.* **261,** 9070–9076
47. Sackett, D. L. (1995) in *Proteins: Structure, Function, and Engineering* (Biswas, B. B., and Siddhartha, R. eds) pp. 255–302, Plenum Press, New York
48. Sackett, D. L. (1995) *Biochemistry* **34,** 7010–7019
49. Bai, R., Pei, X.-F., Boye, O., Getahun, Z., Grover, S., Bekisz, S., Nguyen, N. Y., Brossi, A., and Hamel, E. (1996) *J. Biol. Chem.* **271,** 12639–12645
50. Sawada, T., Kobayashi, H., Hashimoto, Y., and Isawaki, S. (1993) *Biochem. Pharmacol.* **45,** 1387–1394
51. Sackett, D. L., and Varma, J. K. (1993) *Biochemistry* **32,** 13560–13565
52. Little, M., and Luduena, R. F. (1987) *Biochim. Biophys. Acta* **912,** 28–33
53. Luduena, R. F., and Roach, M. C. (1991) *Pharmacol. Ther.* **49,** 133–152